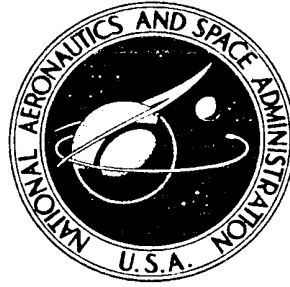


NASA TECHNICAL NOTE



NASA TN D-3364

NASA TN D-3364

FLIGHT MEASUREMENTS OF BOUNDARY-LAYER NOISE ON THE X-15

by Thomas L. Lewis and Norman J. McLeod

*Flight Research Center
Edwards, Calif.*

NASA TN D-3364

FLIGHT MEASUREMENTS OF BOUNDARY-LAYER NOISE ON THE X-15

By Thomas L. Lewis and Norman J. McLeod

**Flight Research Center
Edwards, Calif.**

NATIONAL AERONAUTICS AND SPACE ADMINISTRATION

**For sale by the Clearinghouse for Federal Scientific and Technical Information
Springfield, Virginia 22151 - Price \$0.20**

FLIGHT MEASUREMENTS OF BOUNDARY-LAYER NOISE ON THE X-15*

By Thomas L. Lewis and Norman J. McLeod
Flight Research Center

SUMMARY

Boundary-layer-noise data measured in flight with the X-15 airplane over a Mach number range from 1.0 to 5.4 and at altitudes from 45,000 feet to 105,000 feet are presented. The data were obtained at four locations on the airplane, selected to provide varied boundary-layer conditions. The highest recorded noise level was 150 decibels. Boundary-layer parameters were measured at one location and are used to present the noise data in a nondimensional form for comparison with data from flat-plate wind-tunnel studies by other experimenters.

An appendix is included which illustrates the sensitivity of the microphones used to obtain the data as they are affected by altitude, vibration, and transient heating.

INTRODUCTION

An important aspect of research on boundary-layer flow is the noise generated in the boundary layer by fluctuating pressures. One of the factors affected by the fluctuating pressures is structural weight. This effect is demonstrated by use of a simplified structure, as illustrated in figure 1 (taken from ref. 1). In this example, the skin thickness required for adequate fatigue life in an acoustic environment is shown. The schematic diagram at the lower right illustrates the structure. The results presented show that an increase of sound level from 115 dB to 125 dB would require an increase in skin thickness from 0.03 inch to about 0.06 inch. An increase in rib thickness is also required to withstand the more severe environment. This increase of 10 decibels in sound level would result in a structural weight increase of at least 75 percent.

Noise levels shown in this example are lower than may be encountered in flight, but the curve clearly indicates that, for higher noise levels, the increase in weight will be greater. Also, acoustic insulation necessary for passenger comfort will increase the weight.

Graphs of this type established on the basis of ground tests might be used in the design of aircraft structures if the noise levels could be predicted for

*This paper was included in a classified report entitled "Fourth Conference on Progress of the X-15 Research Airplane Program," Flight Research Center, Oct. 7, 1965. NASA SP-90, 1965. An appendix has been added to describe the instrumentation, and its frequency response, that was used in obtaining the data.

new flight regimes. Unfortunately, the state of the art leaves much to be desired in this respect, and the designer must rely on measured noise data. In the past, only a few in-flight measurements of boundary-layer noise over a significant range of flight conditions have been taken.

The X-15 offers the capability of obtaining noise data over a wide range of dynamic pressure and Mach number that exceeds those available from the flight envelopes of present and proposed aircraft up to Mach 6.

SYMBOLS

C_{f_i}	incompressible skin-friction coefficient
dB	decibels ($\text{dB} = 20 \log_{10} \frac{\sqrt{p^2}}{\sqrt{p_o^2}}$, where $\sqrt{p_o^2} = 4.177 \times 10^{-7}$ pounds per square foot)
g	acceleration due to gravity, feet per second ²
h_p	altitude, feet
l	rib spacing, inches
M	Mach number
$\sqrt{p^2}$	root-mean-square value of pressure fluctuations (sound level), pounds per square foot
$\overline{p^2(\omega)}$	mean-square pressure fluctuation per unit bandwidth, defined by $\overline{p^2} = \int_0^\infty \overline{p^2(\omega)} d\omega$, lb ² sec/ft ⁴
q	dynamic pressure, pounds per square foot
R_θ	Reynolds number based on momentum thickness
t_s	skin thickness, inches
U	local velocity outside boundary layer, feet per second
β	constant of proportionality
δ^*	boundary-layer displacement thickness, feet
ω	frequency, radians per second
Subscript:	
∞	refers to free-stream conditions
2	

INSTRUMENTATION

For the boundary-layer-noise experiments on the X-15 airplane, five locations were selected to obtain data. These locations are shown in figure 2 (from ref. 2). Location 5 was recently chosen for investigation because a large amount of boundary-layer information on heat transfer and skin friction has been obtained at this location as reported in reference 3. As yet, however, no noise data have been obtained here.

At present, flow measurements have been taken only at location 1. A sketch of the test panel used for the study is shown in figure 3. On the forward end of the panel is a mounting block which holds the microphone and temperature-sensing elements. These temperatures are used for microphone calibration. An accelerometer that was attached to the back of the mounting block was used to verify that no corrections were necessary to the acoustic data because of vibrations. To the rear of the microphone are a boundary-layer rake and a static-pressure orifice to determine local flow conditions.

All noise, acceleration, and pressure data were recorded on an onboard tape recorder, and temperature was recorded on an oscillograph.

The microphones were calibrated for linearity, frequency response, the effect of altitude, steady-state temperatures, and transient temperatures. These calibrations resulted in an estimated accuracy of ± 3 dB over a frequency range from 50 to 10,000 cycles per second for all flight conditions. The frequency response of the microphones and the results of the transient heating tests are presented in the appendix.

RESULTS AND DISCUSSION

Test conditions for a typical X-15 flight made primarily to obtain boundary-layer noise data are shown in figure 4. The vehicle was launched at an altitude of 45,000 feet, was accelerated to a Mach number of 5.4, and attained a maximum altitude of 105,000 feet. The maximum free-stream dynamic pressure is shown to be approximately 1000 pounds per square foot. It should also be mentioned that during the portion of the flight where Mach number and dynamic pressure are changing slowly, the angle of attack was relatively constant. The purpose of this flight profile was to keep the environment from changing too rapidly.

Data illustrating how the noise varied at different points on the airplane during this flight are presented in figure 5. Time histories of the sound level in decibels are shown only for locations 1 to 4 (indicated in fig. 2). The times for launch, engine burnout, and Mach 1 during deceleration are marked on the abscissa in figure 5.

Noise levels for the two midfuselage stations (locations 1 and 2) are illustrated by the solid and dashed lines, for the aft fuselage station (location 3) by the upper line, and for the base region (location 4) by the lower

line. For the most part, there is a spread of only 20 decibels in the levels-- but this spread means that the highest sound levels recorded are ten times the lowest, which illustrates the range of the designers' problems. Note also the sudden jump in the traces for locations 3 and 4 when the speed brakes were extended. This result shows that protuberances on the surface of the vehicle can cause large increases in the noise level.

Although the overall sound levels are important, the distribution of the sound in frequency bands is also important, as is shown in figure 6. For these data, the free-stream Mach number was 5.2 and the dynamic pressure was 380 pounds per square foot. The sound level is shown in decibels for the overall noise and for each octave band (center frequencies from 63 to 8000 cps). Locations 1 and 3, which are on the lower surface of the side fairings, have the highest sound levels, particularly at the higher frequencies. Location 2 on the upper side fairing has its highest noise level predominantly at the lower frequencies. The spectrum for location 4 on the left blowout panel is lower in each octave band and is approximately flat.

In order to examine the effect of compressibility on boundary-layer noise, figure 7 shows a comparison of X-15 data with subsonic data obtained by other experimenters (refs. 4, 5, and 6). For this comparison the data from location 1 are examined. For the X-15 data, an equivalent-flat-plate incompressible skin-friction coefficient was calculated by using Blasius' formula with the measured-momentum-thickness Reynolds number.

According to reference 4, Kraichnan's analysis of the boundary layer on a flat plate indicated the proportionality constant β to be in the range from 2 to 12. Wind-tunnel investigations at low speed have given values from 2.5 to 4.8. The X-15 data indicate values from 2 to 4.6 and show a tendency to decrease slightly with increasing Mach number. (Because this is an equivalent-flat-plate comparison, only X-15 data which closely approximate these conditions are shown.) The results indicate that the general levels of this dimensionless coefficient, at this location, are changed very little by effects of compressibility.

Since the comparison between data from wind tunnel at subsonic speeds and from flights at high supersonic speeds shown in this figure deals only with the overall sound pressure, it is of interest to compare the frequency content. Willmarth, Serafini, and others (refs. 4 to 7) have shown that the noise power in the frequency bands can be normalized in terms of the boundary-layer displacement thickness and local free-stream velocity. This procedure has been applied to some of the X-15 data. The results, presented in figure 8, show that the frequency content of the noise measured in flight is significantly different from the wind-tunnel noise. This difference lies in how the energy is distributed over the frequency range. The flight data have more energy at the low frequencies and less energy at the high frequencies than the wind-tunnel data. Even though the data are for two widely different Mach numbers, it cannot be concluded at this time that the difference can be attributed entirely to Mach number, since it is known that the X-15 surface has considerable roughness. In boundary-layer flow, the effects of surface roughness, typical of flight vehicles, perturbs the boundary-layer pressure fluctuations in the lower frequencies even at subsonic speeds.

The results in figures 7 and 8, although somewhat preliminary, show that the theory of Kraichnan (as given in ref. 4), supported by wind-tunnel measurements at subsonic speeds, can be used to estimate the total noise expected on a hypersonic flight vehicle but it does not give a true picture of the energy distribution that is important for design.

CONCLUDING REMARKS

Flight results from boundary-layer noise measurements at specific locations on the X-15 have been presented and a limited comparison with analytical equivalent flat-plate results made. These results indicate that more extensive flight measurements are required to establish a guide for the theoretical studies and laboratory tests that are necessary to define the characteristics of boundary-layer noise.

Continued effort in the X-15 boundary-layer-noise program is necessary to provide for the extension of the range of the present data, as well as to permit a comprehensive analysis of the noise at other locations, particularly on the vertical tail where data can be obtained that can be favorably compared with flat-plate experiments of other investigations.

Flight Research Center
National Aeronautics and Space Administration
Edwards, Calif., October 7, 1965.

APPENDIX

BOUNDARY-LAYER-NOISE INSTRUMENTATION

The instrumentation panel used for obtaining surface-pressure fluctuations and local-flow measurements at location 1 is shown in figure 3. The noise data and the local-flow data were recorded in the vehicle on a miniature airborne tape recorder using 1.5 mil, 1-inch tape at 15 in./sec. Noise data were recorded on direct record, and the flow data were FM multiplexed. The temperature data were recorded on an oscillograph.

A 1/2-inch Photocon microphone (model 504), of the condenser type with a diaphragm recessed below a perforated cap, was used. The microphone was mounted in a heavy mounting block with the cap flush to the surface of the vehicle. This method of mounting results in an orientation such that the microphone diaphragm is generally parallel to the thrust axis of the vehicle for locations 1, 2, and 3. The microphone diaphragm for location 4 was perpendicular to the thrust axis. The response of the microphones at high altitude was determined by an electrostatic actuator in a vacuum chamber. The results of this test, obtained by methods presented in reference 8, are shown in figure 9.

In order to assess the vibration sensitivity of the microphones, they were placed in an electromagnetic shaker and vibrated perpendicular to the diaphragm from 0.25g to 3g in 0.25g steps over the entire response range. The output for a vibration test at 3g is shown in the left plot of figure 10, and the output at 500 cps over the entire range of vibration is shown in the right plot.

The effect of temperature on the microphones has also been determined. The response change of the microphones after being soaked for 30 minutes at constant temperatures is shown in figure 11. To determine the effect of transient heating, the microphones were also heated using a temperature time history, taken from data recorded in flight on a thermocouple located directly below the perforated cap of the dummy microphone. Using a 1000-cps, 120-dB sound source (30 dB above ambient and without anechoic chamber), the response was found to drift less than ± 1 dB as the temperature changed from -40° F to 320° F, as is shown in figure 12. The dummy-microphone thermocouples were used to insure the same heating rates as recorded in flight during this test.

It can be seen that transient heating causes a smaller change at the 1000-cps frequency than the constant temperature frequency response shows. This difference is due to expansion effects on the diaphragm while heat is applied. It is believed that a transient heating response best applies to these X-15 data, thus no correction was applied to the data presented. However, the noted accuracy of ± 3 dB includes the effect of transient heating.

REFERENCES

1. Hubbard, Harvey H.; Edge, Philip M., Jr.; and Modlin, Clarence T., Jr.: Design Considerations for Minimizing Acoustical Fatigue in Aircraft Structures. WADC-University of Minnesota Conference on Acoustical Fatigue, W. J. Trapp and D. M. Forney, Jr., eds., WADC Tech Rep. 59-676, U.S. Air Force, March 1961, pp. 321-338.
2. Kordes, Eldon E.; and Tanner, Carole S.: Preliminary Results of Boundary Layer Noise Measured on the X-15 Airplane. Acoustical Fatigue in Aerospace Structures. Walter J. Trapp and Donald M. Forney, Jr., eds., Syracuse University Press, May 1964, pp. 85-96.
3. Banner, Richard D.; and Kuhl, Albert E.: A Summary of X-15 Heat-Transfer and Skin-Friction Measurements. NASA TM X-1210, 1966.
4. Serafini, John S.: Wall-Pressure Fluctuations and Pressure-Velocity Correlations in a Turbulent Boundary Layer. NASA TR R-165, 1963.
5. Willmarth, William W.: Wall Pressure Fluctuations in a Turbulent Boundary Layer. NACA TN 4139, 1958.
6. Willmarth, W. W.: Space-Time Correlations and Spectra of Wall Pressure in a Turbulent Boundary Layer. NASA MEMO 3-17-59W, 1959.
7. Lilley, G. M.; and Hodgson, T. H.: On Surface Pressure Fluctuations in Turbulent Boundary Layers. AGARD Rep. 276, April 1960.
8. Beranek, Leo L.: Acoustic Measurements. John Wiley & Sons, Inc., July, 1962.

EFFECT OF NOISE ON SKIN THICKNESS

EXAMPLE FOR TYPICAL SKIN-STRINGER CONSTRUCTION

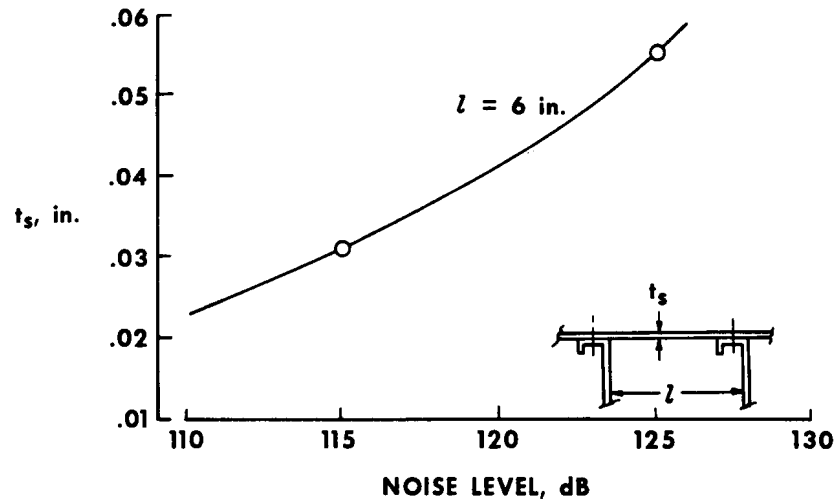


Figure 1

MICROPHONE LOCATIONS ON THE X-15

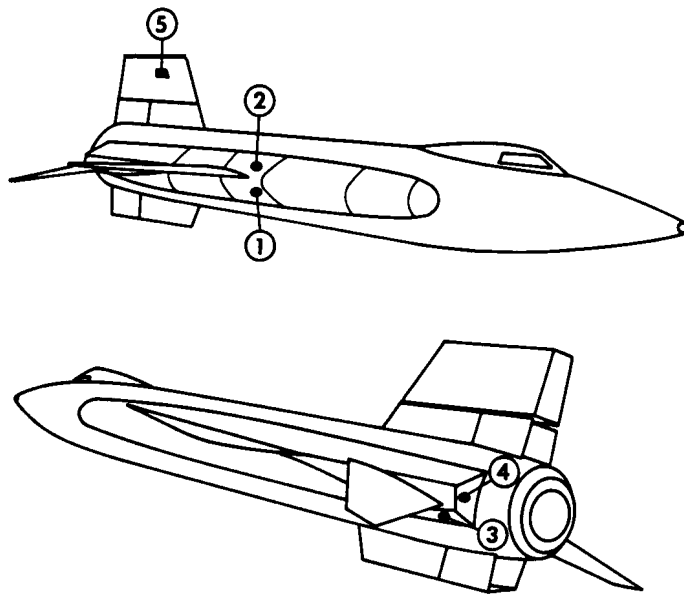


Figure 2

BOUNDARY-LAYER-NOISE TEST PANELS

LOCATION 1 (RIGHT SIDE FAIRING)

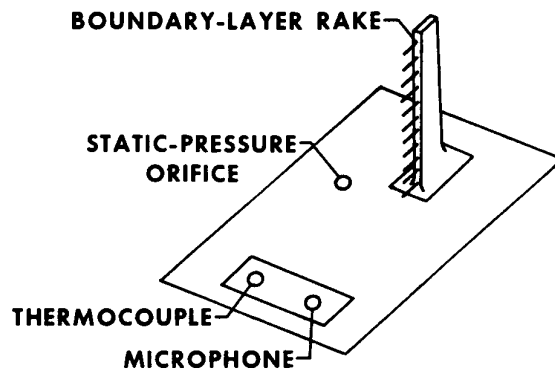


Figure 3

TYPICAL FLIGHT CONDITIONS FOR MEASUREMENT OF X-15 BOUNDARY-LAYER NOISE

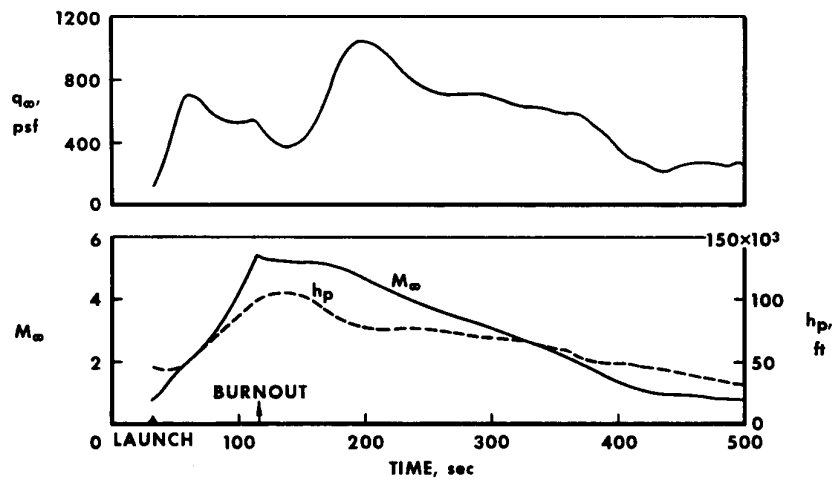


Figure 4

BOUNDARY-LAYER-NOISE DATA FOR FOUR LOCATIONS

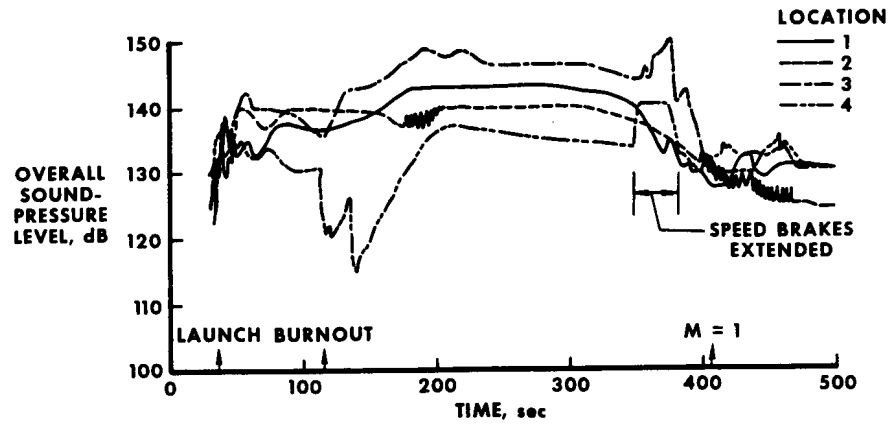


Figure 5

SOUND SPECTRUM FOR FOUR LOCATIONS

$M_\infty = 5.2$; $q_\infty = 380$ psf

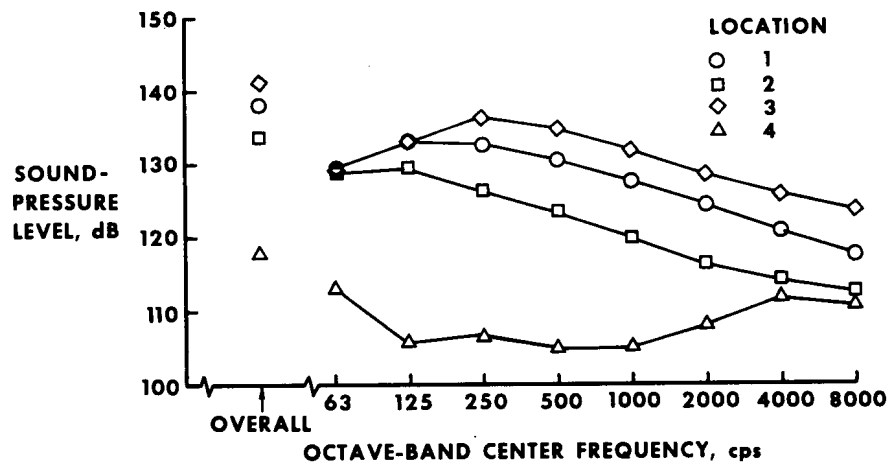


Figure 6

EFFECT OF COMPRESSIBILITY ON OVERALL SOUND-PRESSURE LEVEL

$$\left[\frac{\sqrt{p^2}}{q} = \beta c_{f_i} \right]$$

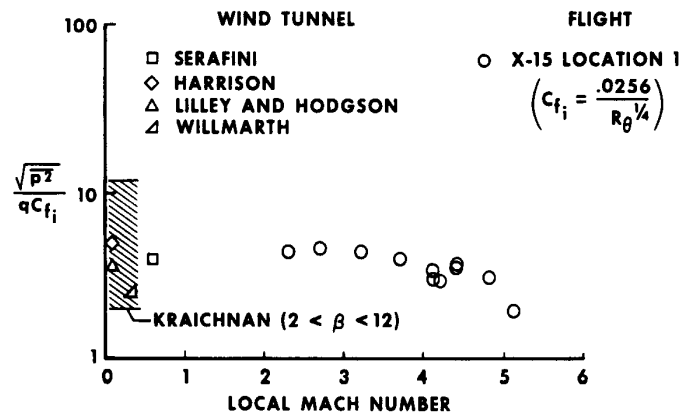


Figure 7

MEAN-SQUARE SPECTRA OF BOUNDARY-LAYER PRESSURE FLUCTUATIONS

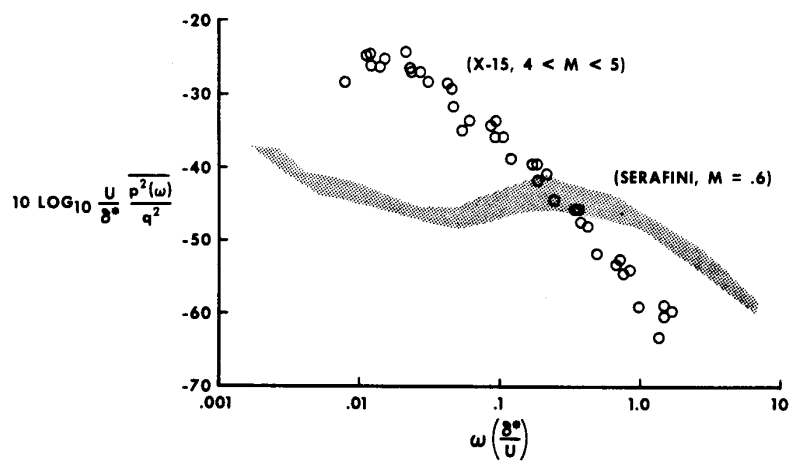


Figure 8

MICROPHONE-RESPONSE CHANGE AT VARIOUS ALTITUDES

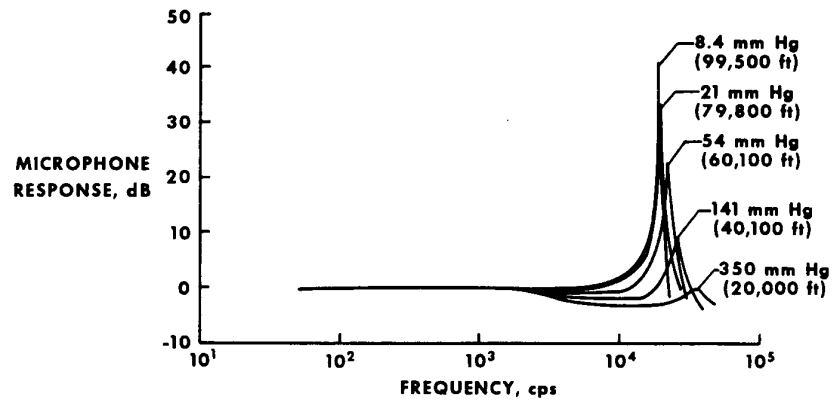


Figure 9

MICROPHONE VIBRATION TESTS

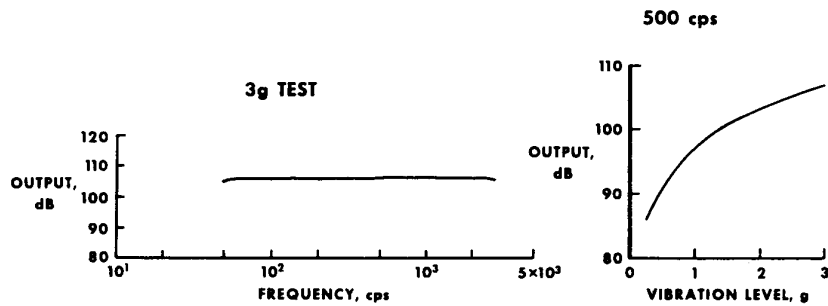


Figure 10

RESPONSE CHANGE AT VARIOUS CONSTANT TEMPERATURES

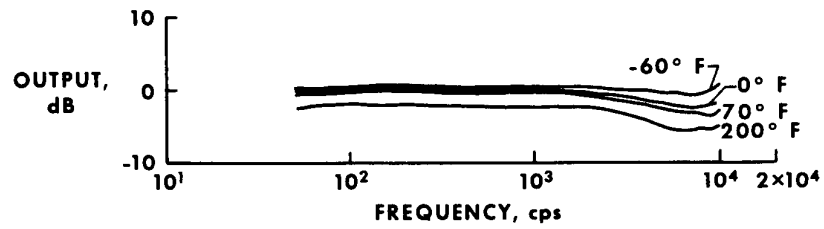


Figure 11

RESPONSE CHANGE DURING TRANSIENT HEATING TESTS

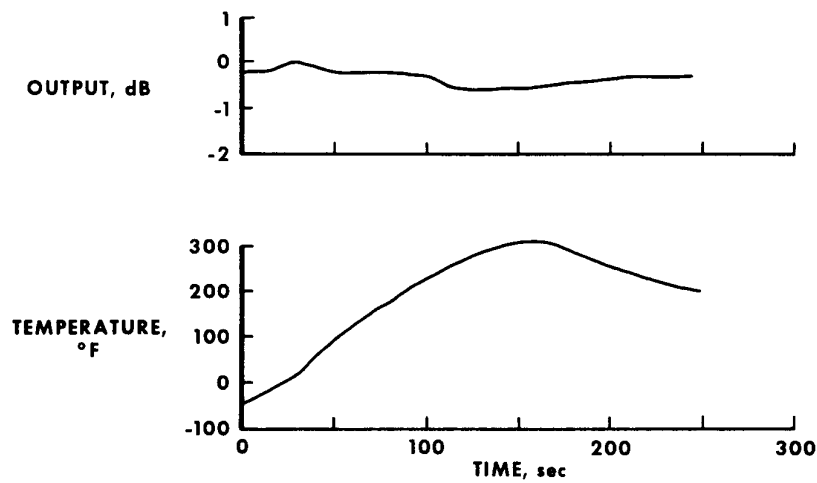


Figure 12